Long-term behavior of GFRP reinforcing bars

Tommaso D'Antino[1*], Marco A. Pisani[1]

[1]Politecnico di Milano, Department of Architecture, Built Environment and Construction Engineering, Piazza Leonardo da Vinci 32, 20133 Milan, Italy

Abstract

Glass fiber reinforced polymer (GFRP) bars represent a valid solution as internal reinforcement of concrete members for some particular applications. GFRP reinforcing bars (rebars) have a high-strength-to-weight ratio and good resistance to corrosion. However, they may suffer of degradation when exposed to specific aggressive environments and when subjected to long-term sustained stress. To increase their durability, design guidelines available in the literature limit the stress level in the rebar. However, such limitations are based on few experimental results and represent conservative estimation of the bar long-term behavior. In this paper, the results of 9 short-term tensile tests and 17 long-term tensile tests on GFRP bars are presented. The long-term tests included relaxation and creep tests for 1000 and 2000 hours considering five different initial applied stress levels. The results obtained are described by two new relaxation and creep functions able to reproduce the bar behavior from the application of the initial applied stress. The functions proposed allow for obtaining the long-term relaxation losses of the reinforcing bars for different stress levels.

Keywords: GFRP bars; creep; relaxation; long-term behavior; experimental tests.

*Corresponding author: tommaso.dantino@polimi.it

1 Introduction

In the last few decades, the use of fiber reinforced polymer (FRP) composites has become a common practice in the civil engineering industry due to some advantages associated with the use of these composites, such as their high strength-to-weight ratio and good resistance to corrosion. FRP composites are generally employed as externally bonded reinforcement (EBR) of existing structural members [1] or as internal reinforcement of new concrete members [2], although other types of application can be found in the literature [3]. When employed as internal reinforcement of concrete members, glass fiber reinforced polymer (GFRP) reinforcing bars (referred to as rebars in this paper) are generally preferred to other types of bar due to their good mechanical properties, resistance to corrosion, and low price. Since they do not suffer from corrosion, GFRP rebars allow for increasing the service life of concrete members in various unfavorable conditions ([4], [5], [6]). However, GFRP rebars represent a relatively new material in the construction field and, although some design guidelines are available in the literature ([7], [8], [9]), further studies are needed to fully understand the behavior of these composites with respect to various applications.

One of the main concerns associated with the use of GFRP rebars is their long-term behavior with respect to different exposure environments and applied loads. Numerous research groups investigated the effect of certain aggressive exposures (e.g. humidity, alkaline solutions, salt solutions, high temperature, etc.) on the long-term behavior of GFRP rebars reporting significant reductions of the bar tensile strength in some cases [10]. The exposure to alkaline environments was reported to be the most aggressive condition, which led to residual tensile strength values equal to approximately 20% of the corresponding short-term unconditioned tensile strength f_f [11].

Furthermore, the contemporary presence of sustained stress and aggressive environmental conditions may affect the GFRP long-term behavior (see for instance [12]). Although some studies observed that the degradation of the GFRP properties is accelerated by the presence of sustained loads in the bar [13], this circumstance is not always confirmed ([14], [15]). However, the presence of sustained loads is responsible for an increase of the bar longitudinal deformation with time. This phenomenon, i.e. the progressive deformation with time under constant load, is known as creep. Similarly, the decay in stress with time when the material is kept under constant strain is referred to as relaxation. Creep and relaxation laws are employed to describe the long-term behavior of various structural materials. Polymeric (organic) resins present a viscoelastic behavior and report considerable creep deformations that depend on the exposure temperature ([16], [17]). Analogously, concrete is a viscoelastic material and its behavior under long-term loads can be described by means of creep laws ([18], [19], [20], [21], [22]), whereas the long-term behavior of prestressing steel tendons is usually described through relaxation laws ([18], [19], [21], [23]).

When FRP rebars are subjected to long-term high applied loads (above the "moderate stress limit" [13]), progressive rupture of the fiber filaments with consequent failure of the bar may occur. To prevent the occurrence of such type of failure, which is referred to as creep rupture or static fatigue ([24], [25], [26]), the Canadian [7], Italian [8], and American [9] design guidelines for GFRP reinforcing bars conservatively limit the maximum stress in the bar under service loads to $0.25f_f$, $0.30f_f$, and $0.20f_f$, respectively. Although these stress limits may seem quite restrictive, they represent reasonable stress values under service load of GFRP rebars reinforcing concrete members [27]. Indeed, due to their low elastic modulus, GFRP rebars shall have low tensile stresses under service load to limit the member deflection [14] and hence guarantee the integrity of the superstructures.

The available literature shows that the study of the long-term behavior of GFRP rebars is of fundamental importance to correctly design GFRP-reinforced concrete members. This paper presents the results of 9 short-term tests and 17 long-term (relaxation and creep) tests conducted on GFRP reinforcing bars. Three groups of rebars with different characteristics were provided by the same manufacturer. The rebars were subjected to five different initial applied stresses, namely $0.1f_f$, $0.2f_f$, $0.4f_f$, $0.6f_f$, and $0.8f_f$, where f_f is the bar short-term tensile strength of the corresponding bar group, for 1000 hours (15 tests) and 2000 hours (2 tests), which are the test durations generally required for common seven wire steel strands [23]. Two new relaxation and creep functions are proposed and calibrated employing the experimental results. The relaxation and creep functions proposed provided accurate results for the entire test duration, i.e. from the application of the initial applied stress, and can be used to estimate the long-term relaxation losses of the reinforcing bars for different stress levels.

2 Experimental campaign

Twenty-six GFRP rebars coming from the same manufacturer and with nominal diameters of 12.0 mm (8 rebars) and 12.5 mm (18 rebars) were tested. The rebars were divided in three groups, two (group 1 and 2) comprising n=8 rebars each and one (group 3) n=10 rebars. Each group is associated with a single production batch, which guarantees the homogeneity of the specimens within each group. For each group, three rebars were subjected to quasi-static tests to determine their mechanical properties whereas the remaining rebars were subjected to relaxation or creep tests with different durations, as explained in the following sections.

2.1 Properties of the rebars

All GFRP rebars were coated with coarse quartz sand embedded in the resin on the bar surface. Rebars of groups 2 and 3 were also helically wrapped with an aramid yarn (see Figure 1 that shows a photo of rebars in group 3). The nominal diameter, density, fiber content, mean glass transition temperature T_g, and bond strength of each rebars group were provided by the manufacturer and are listed in Table 1.

Table 1. Properties of the GFRP rebars.

Group	n [-]	Nominal diameter [mm]	Density (ASTM D792	Fiber content (ASTM	Mean T_g (ASTM E 1356*	Bond strength (ASTM D7913/D7913M† [31]) [MPa]	Average tensile strength f_f	Average elastic modulus

			[28])	D2584	[30])		[32]	E [32]
			[g/cm^3]	[29]) [%]	[°C]		[MPa]	[MPa]
1	8	12.0	1.95	>65	>100	>7.6	1000^{+}	>44800
2	8	12.5	1.95	>65	>100	>7.6	885^{+}	>44800
3	10	12.5	1.95	>65	>100	>7.6	1050^{+}	47484^{+}

*midpoint temperature, see also [33]. †see also [34]. $^{+}$Obtained experimentally.

The rebars average short-term (quasi-static) tensile strength f_f was obtained by quasi-static tensile tests of three rebars from each group according to ASTM D7205 [32]. The results obtained are reported in Table 1, whereas the stress-relative displacement between the grips curves obtained for the three rebars in group 3 are reported in black in Figure 2a. The average tensile strength of group 2 (f_f =885 MPa) is slightly lower than the others because of the tight winding of the aramid yarn in these rebars, which prevented parallelism of the peripheral glass fibers affecting the bar strength. For two of the three rebars subjected to short-term tensile tests in group 3, an extensometer with gauge length 200 mm was employed to measure the bar strain and compute the elastic modulus. The first bar was tested without measuring the strain to avoid possible damage of the extensometer due to the sudden explosive failure expected, since the bar tensile strength was not known in advance. The stress-strain curves obtained are depicted in red in Figure 2a, where the elastic modulus E_0 is also indicated, whereas a photo of the rebars failure is reported in Figure 2b. It should be noted that these curves do not attain the tensile strength because the extensometer was removed at approximately half of the tensile strength measured on the first bar to avoid possible damage of the instrument. The average elastic modulus $\bar{E}_0 = 47.5$ GPa obtained from the experimental tests of group 3 bars and those provided by the manufacturer for groups 1 and 2 are reported in Table 1.

2.2 Relaxation and creep tests

The first two groups of specimens were subjected to relaxation tests for 1000 hours. The tests were carried out using an electromechanical testing machine designed to determine the relaxation loss of steel wires and strands (Figure 3). This machine maintains the strain constant with time by modifying the load applied to the specimen. The strain is constantly measured by an extensometer with gauge length 400 mm attached to the specimen and connected to the controlling software that compensates for elongations of the specimen by moving a weight on a lever arm of the testing machine. The testing machine is placed in an air-conditioned room with controlled temperature (20±1°C) and humidity (RH=50±1%). Each specimen was stored for at least one week in this room before starting the test. The calibration of all the instrumentation was checked before starting the tests.

The specimens were named following the notation TPSDZ, where T indicates the type of test (C=creep test, R=relaxation test), P indicates the percentage of stress with respect to the strength f_f of the rebar at the beginning of the test (10=0.1f_f, 20=0.2f_f, 40=0.4f_f, 60=0.6f_f, and 80=0.8f_f, see Table 1), S indicates whether the rebar is helically wrapped (S=H) or not (S=N), D indicates the duration of the test (1=1000 hours, 2=2000 hours), whereas Z is the specimen number. All specimens are reported in Table 2.

Table 2. Specimens subjected to relaxation and creep tests.

Name	Group	Type	Duration [hours]	Initial applied stress [%]	$J(t-t_0)\cdot E$ ($t-t_0$=100 years)
R10N1A	1	Relaxation	1000	10	1.0718
R20N1A	1	Relaxation	1000	20	1.0628
R40N1A	1	Relaxation	1000	40	1.1222
R60N1A	1	Relaxation	1000	60	1.1516

R60N1B	1	Relaxation	1000	60	1.1396
R10H1A	2	Relaxation	1000	10	1.0456
R20H1A	2	Relaxation	1000	20	1.0659
R40H1A	2	Relaxation	1000	40	1.0552
R40H1B	2	Relaxation	1000	40	1.1396
R60H1A	2	Relaxation	1000	60	1.1422
C20H1A	3	Creep	1000	20	1.1057
C40H1A	3	Creep	1000	40	1.1052
C40H2A	3	Creep	2000	40	1.0851
C60H1A	3	Creep	1000	60	1.0459
C60H2A	3	Creep	2000	60	1.0658
C80H1A	3	Creep	1000*	80	-
C80H1B	3	Creep	1000†	80	-

Note: *Failure occurred after 370 minutes. †Failure occurred after 455 minutes.

The results obtained by the 10 specimens in groups 1 and 2 are reported in Figure 4, where $(t-t_0)$ is the elapsed time between the time of first loading t_0 and the current time (i.e. the time in which the measurement is taken). The axial force-elapsed time curves show some irregularities (i.e. abrupt changes of load) due to difficulties in the automatic adjustment of the load by the machine. These difficulties are caused by the inherent characteristics of the machine, which was designed for relaxation and creep tests of steel specimens. In fact, glass FRP rebars have a stiffness lower than that of steel wires and strands and the weight moving quickly on the lever arm sometimes caused dynamic effects that could not be controlled by the machine controlling software.

To avoid this problem, the rebars in group 3 were tested under load control (creep tests) using the same machine for 2000 hours (2 tests) and 1000 hours (5 tests). In this case, the strain control was deactivated and the load was corrected manually while the specimen strain was measured using a displacement transducer attached to the bar employing a gauge length of 200 mm (see call-out in Figure 3). Four different initial applied stresses, namely $0.2f_f$, $0.4f_f$, $0.6f_f$, and $0.8f_f$, were considered. The specimens subjected to creep tests are reported in Table 2, whereas the corresponding strain-elapsed time curves are depicted in Figure 5. The strain-elapsed time curves of the two bars subjected to creep test at $0.8f_f$ are not reported in Figure 5 because complete bar failure, i.e. contemporary tensile rupture of all fibers within the cross-section, occurred after 370 minutes (6.17 hours) and 455 minutes (7.58 hours) from the initial applied stress for the two specimens, respectively. These tests clearly indicate that a sustained stress of $0.8f_f$ causes the creep rupture of the GFRP rebar in less than 8 hours. Creep rupture was not observed for specimens with an applied stress up to $0.6f_f$ for up to 2000 hours. However, further studies are needed to investigate the long-term behavior of the rebars with sustained stress between $0.6f_f$ and $0.8f_f$.

Similarly to Figure 4, the strain-elapsed time curves in Figure 5 show stepwise oscillations due to the manual adjustment of the applied stress. However, these oscillations did not hinder the definition of the creep functions, as discussed in Section 3. Figure 4 and Figure 5 show that the axial force measured at the time of first loading t_0 and the instantaneous (elastic) strain, respectively, of some nominally equal tests are different. These differences could not be attributed either to a possible loss of calibration of the machine with time, which was verified, or to inhomogeneity in the stiffness of the specimens, which was not observed in quasi-static tensile tests of specimens from the same batch. They are then attributed to the loading operation that was performed manually and took approximately 10 minutes. Indeed, during this initial loading procedure, significant creep deformations may occur since changes of the load rate affect the total deformation, which includes both the instantaneous elastic and creep deformations. As a result, the strain measured at the initial applied load of specimens in Figure 4 and Figure 5 was slightly different (differences lower than 5%) than the strain associated to the same load according to the bar mechanical properties reported in Table 1, except for specimen C40H2A, which reported an initial strain 12% lower than the corresponding short-term strain.

The occurrence of significant creep deformation at the beginning of the test is also confirmed by the percent stress losses $100\cdot[\sigma(t_0)-\sigma(t)]/\sigma(t_0)$ ($\sigma(t_0)$ is the stress at the time of loading t_0) of relaxation tests, which are depicted in Figure 6 and show the maximum effect of creep in the initial phase of the test. Figure 6 also shows inhomogeneity of the rheological behavior of the specimens: the percent stress loss does not always increase with the initial stress level and this behavior is similar for both groups of specimens. This phenomenon will be discussed in detail in Section 4.

2.3 Tensile tests after creep tests

After the long-term creep tests, all rebars of group 3 were subjected to quasi-static tensile tests to determine the residual tensile strength and elastic modulus. The results obtained, which are reported in Table 3 for each bar, indicate that the bar tensile strength is not affected by a long-term stress that does not exceed 60% of the corresponding short-term tensile strength f_f. This observation is confirmed by the results of a statistical analysis performed on several GFRP rebars subjected to long-term sustained stress and exposed to different environmental conditions collected from the literature [14].

Table 3. Residual tensile strength and elastic modulus measured after long-term tests of bars in group 3.

Name	Ultimate load [kN]	Tensile Strength [MPa]	Average tensile strength [MPa]	Elastic modulus [MPa]	Average elastic modulus [MPa]
C20H1A	128.7	1049	1049	47407	47407
C40H1A	131.4	1071	1088	47138	47508
C40H2A	135.6	1105		47877	
C60H1A	131.6	1072	1102	45573	46862
C60H2A	138.9	1132		48151	

Moreover, when the long-term stress does not exceed 40% of the short-term tensile strength, the elastic modulus does not vary with the duration of the long-term test. However, the elastic modulus of C60H1A is lower than all other elastic moduli measured (see Figure 2a and Table 3), which confirms the dependency of the elastic modulus on the level and the duration of long-term loading reported in the literature [35]. It should be noted that this dependency is denied by C60H2A, which provided and elastic modulus, measured after a 2000 hours long test, higher than the highest elastic modulus measured on rebars not subjected to long-term tests (Table 1).

In the following, two new analytical relaxation and creep functions (namely Eqs. (5) and (9)) that consider an elastic modulus of the bar E independent of the time of loading are proposed to model the long-term behavior observed experimentally.

3 Analytical relaxation and creep functions

When the percent stress loss-elapsed time curves depicted in Figure 6 are plotted in semi-logarithmic scale, they resemble approximately straight lines (Figure 7). This observation suggests the adoption of a linear function to describe the relaxation of the rebars:

$$\frac{\sigma(t_0)-\sigma(t)}{\sigma(t_0)}\cdot 100 = A + B\cdot \log_{10}\left(t-t_0\right) \tag{1}$$

Note that adopting this equation entails the relaxation law be hereditary, i.e. it is independent of the age of the material. This assumption is wrong when studying the long-term properties of concrete (for which t_0 is the age of concrete at first loading and t is its current age) but is generally adopted in the case of composite materials (see for instance [36] and [37]). Therefore, only the elapsed time (t-t_0) is needed to analyze the long-term behavior of the bars.

Polymers behave in a linear viscoelastic manner when the applied stress level is low [36], whereas glass and carbon fibers do not exhibit significant creep deformations [38]. Therefore, the superposition principle can be employed to describe the stress evolution under variable strain ([39], [40]):

$$\sigma(t) = \varepsilon(t_0) \cdot R(t - t_0) + \int_{t_0}^{t} \frac{d\varepsilon(\tau)}{d\tau} R(t - \tau) \cdot d\tau \qquad (2)$$

where $R(t - t_0)$ is the relaxation function.

When setting $\varepsilon(t_0) = \varepsilon_0 = \cos t$, Eq. (2) can be written in the following form:

$$\begin{aligned} &\sigma(t) = \varepsilon_0 \cdot R(t - t_0) = \varepsilon_0 \cdot E \cdot R(t - t_0) / E = \\ &= \sigma(t_0) \cdot R(t - t_0) / E \quad \Rightarrow \quad R(t - t_0) / E = 1 - \frac{\sigma(t_0) - \sigma(t)}{\sigma(t_0)} \end{aligned} \qquad (3)$$

where E is the elastic modulus measured under a short-term increasing load. Considering Eq. (1), Eq. (3) can be written as:

$$R(t - t_0) / E = 1 - \left[A + B \cdot \log_{10}\left(t - t_0\right)\right] / 100 \qquad (4)$$

It should be noted that Eq. (1) fails to describe the relaxation function of the rebars for all times t because when $t=t_0$ (i.e. at first loading) it should hold $R(t - t_0) / E = 1$ or $R(t - t_0)\big|_{t=t_0} = E$, as clearly shown by Eq. (2). However, when $t=t_0$, Eq. (4) provides an infinite value of the ratio $R(t - t_0) / E$. Therefore, Eq. (5) is proposed to provide a complete relaxation function able to describe the rebar behavior also at time t_0 (time is in hours):

$$R(t - t_0) / E = 1 - \left[A + B \cdot \log_{10}\left(t - t_0 + 1\right)\right] \cdot \left[1 - e^{-2\left(t - t_0\right)}\right] / 100 \qquad (5)$$

It should be noted that the exponential function $\left[1 - e^{-2(t - t_0)}\right]$ introduced in Eq. (5) affects the results only in the first hours of loading, since it is approximately equal to 1 already after four hours of loading ($\left[1 - e^{-2(t - t_0)}\right]$=0.998 for $(t-t_0)$=3 hours). Therefore, Eq. (5) provides (substantially) the same results of Eq. (4) after the first hours of loading, which confirms the reliability of the proposed Eq. (5) in describing the entire relaxation function.

The percent stress loss-elapsed time curve of each relaxation test depicted in Figure 6 was best fitted using Eq. (5). The analytical curves obtained are depicted in Figure 8, where a good agreement between experimental and corresponding analytical results can be observed.

Similarly to Eq. (2), the superposition principle can be employed to describe the strain evolution under variable stress [36]:

$$\varepsilon(t) = \sigma(t_0) \cdot J(t - t_0) + \int_0^t \frac{d\sigma(\tau)}{d\tau} J(t - \tau) \cdot d\tau \tag{6}$$

where $J(t - t_0)$ is the creep function and τ is the integration variable. As well-known, $J(t - t_0)$ can be computed from $R(t - t_0)$ by solving the Volterra integral equation [39]:

$$\int_0^t \frac{dJ(\tau - t_0)}{d\tau} R(t - \tau) \cdot d\tau = 1 - \frac{R(t - t_0)}{E} \tag{7}$$

and vice-versa, when $R(t - t_0)$ is unknown:

$$\int_0^t \frac{dR(\tau - t_0)}{d\tau} J(t - \tau) \cdot d\tau = 1 - E \cdot J(t - t_0) \tag{8}$$

The expression of $J(t - t_0)$ can therefore be obtained by substituting Eq. (5) into Eq. (7). The solution of the resulting integral was computed by means of the numerical integration procedure described in [41] for all the 10 relaxation tests. The results allowed to construct the curve that describes the creep function associated to each test. As an example, Figure 9 shows the $J(t - t_0) \cdot E$ function obtained by the numerical integration for R40H1B, which was initially loaded at $0.4 f_f$. This function is approximately linear except for the first two hours and this behavior is in agreement with previous observations of the creep behavior of composite materials ([36], [42], [35]). Therefore, the creep function of the GFRP rebars can be conveniently described by Eq. (9) (time is still in hours):

$$J(t - t_0) \cdot E(t_0) = 1 + \left[C + D \cdot \log_{10}\left(t - t_0 + 1\right)\right] \cdot \left[1 - e^{-2(t - t_0)}\right] / 100 \tag{9}$$

where the parameters C and D can be obtained from the experimental or numerical creep function by means of a best fitting algorithm. Analogously to Eq. (5), Eq. (9) describes the bar behavior for the entire test duration, i.e. from the initial load application time t_0. Eq. (9) was used to best fit the $J(t - t_0) \cdot E$ function obtained by numerical integration for R40H1B. The curve provided, depicted in Figure 9, shows a good agreement with the numerical solution of $J(t - t_0) \cdot E$, which confirms the accuracy of Eq. (9) in describing the bar complete creep function. It should be noted that, among the 10 relaxation tests performed, R40H1B provided the worst coefficient of determination associated to the best fitting procedure, equal to 0.999466. Furthermore, Figure 9 confirms that the exponential term in Eqs. (5) and (9) affects only the first hours of loading.

Eqs. (5) and (9) allow for comparing all the experimental tests performed. Eq. (5) can be employed for best fitting the results of the 10 relaxation tests, whereas the results of the 5 experimental creep tests can be best fitted by Eq. (9) and then numerically integrated (by solving Eq. (8)) to determine the corresponding relaxation functions.

4 Remarks on the hypotheses adopted

Figure 10 shows the relaxation functions obtained for all long-term tests presented in this paper that did not fail before the test completion, whereas Table 2 reports the corresponding ratio between the total bar deformation at t=100 years, $\varepsilon(t)$, and the deformation at test initiation, $\varepsilon(t_0)$:

$$\frac{\varepsilon(t)}{\varepsilon(t_0)} = J(t - t_0) \cdot E \tag{10}$$

All these relaxation functions were computed adopting the assumption that the time-dependent behavior of the GFRP rebars is linear, i.e. the hypothesis of linear viscoelasticity was assumed. Although it is well established that “polymers will behave in a linear viscoelastic manner when the applied stress levels are low” [36], the maximum stress value (evaluated as a percentage of f_f) that can be applied to the rebars studied in this paper respecting the linear viscoelasticity hypothesis is not known.

The overall behavior of a composite material depends on the matrix, on the reinforcement, and on the distribution of the reinforcement within the matrix. If the composite viscoelastic behavior is non-linear, then Eq. (2) becomes (see [36] and [39]):

$$\sigma(t) = \varepsilon(t_0) \cdot E + F\left(\varepsilon(t_0)\right) \cdot C(t - t_0) + \int_{t_0}^{t} E \frac{d\varepsilon(\tau)}{d\tau} + \int_{t_0}^{t} C(t-\tau) \cdot \frac{dF(\varepsilon(\tau))}{d\tau} d\tau \tag{11}$$

where $F(\varepsilon(\tau))$ is an experimentally determined function of $\varepsilon(\tau)$, which describes the non-linear relation between the imposed strain and stress relaxation for the rebar considered. Moreover, $C(t-\tau) = R(t-\tau) - E$.

When the strain is constant (i.e. in relaxation tests), Eqs. (2) and (11) become Eqs. (12) and (13), respectively:

$$\sigma(t) = \varepsilon(t_0) \cdot R(t-t_0) \quad (12)$$

$$\sigma(t) = \varepsilon(t_0) \cdot E + F(\varepsilon(t_0)) \cdot [R(t-t_0) - E] \quad (13)$$

Therefore, linear viscoelastic behavior can be assumed when the relaxation losses $\sigma(t) - \sigma(t_0)$ linearly increase with the increase of the initial applied stress, which entails $F(\varepsilon(t_0)) = \varepsilon(t_0)$, whereas non-linear viscoelastic behavior shall be assumed otherwise [39].

Thus, linear viscoelastic behavior implies that the function $R(t-t_0)/E = \sigma(t)/\sigma(t_0)$ be independent of the initial stress level, which means that the dimensionless relaxation curves depicted in Figure 10 should overlap one another.

All curves shown in Figure 7 and Figure 10 have similar slopes. Nevertheless, only certain curves overlap regardless of the initial stress level. The $R(t-t_0)/E$ diagrams (Figure 10a) of the specimens belonging to groups 1 and 2 initially loaded at $0.1f_f$ and $0.2f_f$ and the rebars belonging to group 3 initially loaded at $0.6f_f$ are grouped, which suggests a linear viscoelastic behavior for these specimens (the result variability observed may be attributed to the randomly distributed properties of the rebars, as previously observed in the literature [43]). However, results in Figure 6 (group 1 and 2 rebars) generally showed a percent stress loss $100\cdot[\sigma(t_0)- \sigma(t)]/\sigma(t_0)$ that increased with increasing the initial stress, which indicates the presence of non-linear viscoelastic phenomena. Furthermore, specimens belonging to group 3 initially loaded at $0.6f_f$ provided less relaxation losses than specimens of the same batch initially loaded at $0.4f_f$ (Figure 10).

The $\varepsilon(t)/\varepsilon(t_0)$ ratios provided in Table 2 are plotted in Figure 11 with respect to the different initial applied stresses, provided as percentages of f_f. Also in this case, the results do not clearly indicate the presence of linear or non-linear viscoelasticity. In the case of the bars loaded at $0.4f_f$ in group 3, the 2000 hours-long test provided a total deformation lower than the corresponding 1000 hours-long test (see also Figure 5). The highest $\varepsilon(t)/\varepsilon(t_0)$=1.1516 ratio was obtained by R60N1A initially loaded at $0.6f_f$ for 1000 hours. However, C60H1A, loaded at the same ratio and for the same duration of R60H1A, provided $\varepsilon(t)/\varepsilon(t_0)$=1.0459, which is approximately equal to the ratio $\varepsilon(t)/\varepsilon(t_0)$=1.0456 provided by R10H1A, which was initially loaded at $0.1f_f$ for 1000 hours.

The relaxation tests performed seem to suggest (albeit with some exceptions) that the behavior of the rebars is linear viscoelastic for $\sigma(t_0)/f_f \leq 20\%$, while for $40\% \leq \sigma(t_0)/f_f \leq 60\%$ non-linearity should be accounted for. However, the creep tests (rebars in group 3) did not confirm this observation. In fact, in these tests the relaxation losses for $\sigma(t_0)/f_f \leq 40\%$ are similar to those for $\sigma(t_0)/f_f \leq 20\%$, while specimens with $\sigma(t_0)/f_f \leq 60\%$ showed relaxation losses lower than those of tests with lower initial applied stress. Further tests are needed to clearly identify the presence of linear or non-linear viscoelasticity for the bars considered.

It should be noted, however, that in practice it is not reasonable to allow GFRP bars to be subjected to long-term loads higher than 40% of their short-term strength. In the case of non-prestressed reinforcing bars, the maximum rebar stress under service loads is dictated by the reinforced member stiffness requirements (i.e. deflection control requirements) that, due to the low elastic modulus (with respect to that of steel rebars) of the GFRP rebars, determine a maximum rebar stress lower than $0.25f_f$. This means that the maximum stress in the rebars under only the permanent load is usually lower than $0.15f_f$ ([14], [27]).

In the case of prestressed reinforcing bars/tendons [44], the stiffness of the structural member under service loads is usually independent of the elastic modulus of the prestressing bars (due to the absence of cracking, the reinforced member stiffness is essentially related to the member cross-section geometry and properties). Therefore, the maximum stress in the rebars/tendons under service loads is dictated by the need to guarantee the durability of the GFRP bars/tendons, which is mainly affected by creep rupture phenomena and possible bar deterioration due to the aggressive (alkaline) environment of concrete [14]. According to the current literature ([25], [45]), this stress limit should not exceed 0.4f_f, although available design guidelines suggest more cautious values ([7], [8], [9]). The results obtained in this paper suggest that the hypothesis of linear viscoelastic behavior could be adopted up to $\sigma(t_0)/f_f \leq 40\%$, until further investigations are conducted to clarify this aspect.

5 Conclusions

In this paper, 9 short-term tests and 17 long-term tests on glass fiber reinforced polymer bars were described. The specimens, provided by the same manufacturer, belonged to three different batches and were subjected to short-term tests (9 specimens), relaxation (10 specimens) and creep (7 specimens) tests. The long-term tests were conducted for 1000 and 2000 hours considering five different initial applied stresses, namely 0.1f_f, 0.2f_f, 0.4f_f, 0.6f_f, and 0.8f_f, where f_f is the bar short-term tensile strength of the corresponding batch. Two new relaxation and creep functions were proposed and employed to describe the long-term behavior of the bars considered. The results obtained allowed for drawing the following conclusions:

- Relaxation and creep tests showed scattered results, which are attributed to the randomly distributed properties of the rebars. Therefore, a large number of tests is recommended to obtain reliable long-term behavior results.
- The new relaxation and creep functions proposed overcome the issues associated with the use of the widely adopted linear logarithmic relaxation and creep functions and were shown to provide accurate results for the entire duration of the tests, i.e. from the application of the initial applied stress.
- The long-term tests did not affect the strength and elastic modulus of the GFRP bars when the

initial applied stress did not exceed $0.6f_f$.

- The initial applied stress of $0.8f_f$ adopted for two tests caused complete bar failure in less than 8 hours.
- The highest $\varepsilon(t)/\varepsilon(t_0)$=1.1516 ratio was obtained by a test with $0.6f_f$ for 1000 hours. However, tests on bars of a different group with the same initial applied stress provided lower $\varepsilon(t)/\varepsilon(t_0)$.
- The results suggest that for the bars presented in this study a linear viscoelastic behavior can be assumed under service loads, i.e. when $\sigma(t_0)/f_f \leq 40\%$.

It should be noted that these conclusions apply to the specific bars tested. Experimental tests shall be carried out to evaluate the long-term behavior of rebars coming from different manufacturers. Eqs. (5) and (9) may be employed to fit the results and obtain the complete long-term behavior of the rebars.

Acknowledgments

The authors gratefully acknowledge the support of the Materials Testing Laboratory of Politecnico di Milano that provided the testing machine, Ascon Tecnologic srl that provided the instrument to measure the strains in the creep tests, Sielco Sistemi srl that provided the data acquisition system for the creep tests, and Sireg Geotech srl that provided the GFRP bars.

Data Availability

The raw/processed data required to reproduce these findings cannot be shared at this time as the data also forms part of an ongoing study.

References

[1] C. E. Bakis, L. C. Bank, V. L. Brown, E. Cosenza, J. F. Davalos, J. J. Lesko, S. H. Rizkalla, A. Machida and T. Triantafillou, "Fiber-reinforced polymer composites for construction -

State-of-the-art review," *Journal of Composites for Construction,* vol. 6, no. 2, pp. 73-87, 2002.

[2] H. A. Totutanji and M. Saafi, "Flexural Behavior of Concrete Beams Reinforced with Glass Fiber-Reinforced Polymer (GFRP) Bars," *ACI Structural Journal,* vol. 97, no. 5, pp. 712-719, 2000.

[3] T. D'Antino and M. A. Pisani, "Evaluation of the effectiveness of current guidelines in determining the strength of RC beams retrofitted by means of NSM reinforcement," *Composite Structures,* vol. 167, pp. 166-177, 2017.

[4] C. Klowak, A. Memon and A. Mufti, "Static and fatigue investigation of second generation steel-free bridge decks," *Cement and Concrete Composites,* vol. 28, pp. 890-897, 2006.

[5] A. Mufti and K. Neale, "State-of-the-art of FRP and SHM applications in bridge structures in Canada. Compos Res J 2008;2(2):60–9.," *Composites Research Journal,* vol. 2, no. 2, pp. 60-69, 2008.

[6] F. Rostàsy, "FRP tensile elements for prestressed concrete: state of the art, potentials and limits," in *Fiber-reinforced plastic reinforcement for concrete structures - SP-138,* Farmington Hills, American Concrete Institute, 1993, pp. 347-65.

[7] CAN/CSA-S806-02, Design and Construction of Building Components with Fibre-Reinforced Polymers, Rexdale: Canadian Standards Association, 2012, pp.198.

[8] CNR-DT 203/2006, Guide for the design and construction of concrete structures reinforced with fiber-reinforced polymer bars, Rome: National Research Council, 2006, pp.35.

[9] ACI 440.1R-15, Guide for the design and construction of concrete reinforced with FRP bars, Farmington Hills, MI: American Concrete Institute, 2015, pp. 88.

[10] T. D'Antino, M. A. Pisani and C. Poggi, "Effect of the environment on the performance of GFRP reinforcing bars," *Composites Part B,* no. 141, pp. 123-126, 2018.

[11] Y. Chen, J. F. Davalos and I. Ray, "Durability prediction for GFRP reinforcing bars using short-term data of accelerated aging tests," *Journal of Composites for Construction,* vol. 10, no. 4, pp. 279-286, 2006.

[12] J. A. Gonilha, J. R. Correia and F. A. Branco, "Creep response of GFRP–concrete hybrid structures: Application to a footbridge prototype," *Composites: Part B,* vol. 53, pp. 193-206, 2013.

[13] G. Nkurunziza, B. Benmokrane, A. S. Debaiky and R. Masmoudi, "Effect of sustained load and environment on long-term tensile properties of glass fiberreinforced polymer reinforcing bars," *ACI Structural Journal,* vol. 102, no. 4, pp. 615-621, July-August 2005.

[14] T. D'Antino and M. A. Pisani, "Influence of sustained stress on the durability of glass FRP reinforcing bars," *Construction and Building Materials,* vol. 187, pp. 474-486, 2018.

[15] C. Mias, L. Torres, A. Turon and C. Barris, "Experimental study of immediate and time-dependent deflections of GFRP reinforced concrete beams," *Composite Structures,* vol. 96, pp. 279-285, 2013.

[16] J. D. Ferry, Viscoelastic Properties of Polymers, 3rd edition, New York: John Wiley & Sons Inc., 1980.

[17] M. Emara, L. Torres, M. Baena, C. Barris and M. Moawad, "Effect of sustained loading and environmental conditions on the creep behavior of an epoxy adhesive for concrete structures strengthened with CFRP laminates," *Composites: Part B,* vol. 129, pp. 88-96, 2017.

[18] Eurocode 2: Design of concrete structures - Part 1-1: General rules and rules for buildings (EN 1992-1-1), Bruxelles: European Committee for Standardization, 2005.

[19] A. C. 318, Building Code Requirements for Reinforced Concrete (ACI 318-14) and Commentary (318R-14), Farmington Hills: American Concrete Institute, 2014.

[20] CEB, CEB-FIP Model Code 90 - CEB Bulletin No. 213/214, London: Thomas Telford Ltd., 1993.

[21] fib, fib Model Code for Concrete Structures 2010, Berlin: Ernst & Sohn, 2013.

[22] RILEM TC-242-MDC (Zdeněk P. Bažant chair), "RILEM draft recommendation: TC-242-MDC multi-decade creep and shrinkage of concrete: material model and structural analysis," *Materials and Structures,* vol. 48, no. 4, pp. 753-770, April 2015.

[23] ASTM International, Standard Specification for Low-Relaxation, Seven-Wire Steel Strand for Prestressed Concrete - A416/A416M—18, 100 Barr Harbor Drive, PO Box C700, West Conshohocken, PA 19428-2959. United States: ASTM International, 2018.

[24] L. C. Bank, Composites for Construction: Structural Design with FRP Materials, Hoboken: John Wiley & Sons, 2006.

[25] M. Sayed-Ahmed, B. Hajimiragha, B. Hajimiragha, K. Mohamed and B. Benmokrane, "Creep rupture and creep behaviour of newly third generation GFRP," in *Proceedings of the Fifth International Conference on Durability of FRP Composite for Construction and Rehabilitation of Structures (CDCC-17),* University of Sherbrooke, Quebec, Canada, 2017.

[26] ASTM International, Standard test method for tensile creep rupture of fiber reinforced polymer matrix - D7337/D7337M − 12, 100 Barr Harbor Drive, PO Box C700, West Conshohocken, PA 19428-2959. United States: ASTM International, 2016.

[27] V. Carvelli, M. Pisani and C. Poggi, "Fatigue behaviour of concrete bridge deck slabs reinforced with GFRP bars," *Composites: Part B,* vol. 41, p. 560–567, 2010.

[28] ASTM International, Standard test methods for density and specific gravity (relative density) of plastics by displacement - D792-13, 100 Barr Harbor Drive, PO Box C700, West Conshohocken, PA 19428-2959. United States: ASTM International, 2013.

[29] ASTM International, Standard test method for ignition loss of cured reinforced resins - D2584-18, 100 Barr Harbor Drive, PO Box C700, West Conshohocken, PA 19428-2959. United States: ASTM International, 2018.

[30] ASTM International, Standard test method for assignement of the glass transition temperatures by differential scanning calorimetry - E1356-08, 100 Barr Harbor Drive, PO Box C700, West Conshohocken, PA 19428-2959. United States: ASTM International, 2008.

[31] ASTM International, Standard test method for bond strength of fiber-reinforced polymer matrix composite bars to concrete by pullout testing - D7913/D7913M-14, 100 Barr Harbor Drive, PO Box C700, West Conshohocken, PA 19428-2959. United States: ASTM International, 2014.

[32] ASTM International, Standard test method for tensile properties of fiber reinforced polymer matrix composite bars - D7205/D7205M-06, 100 Barr Harbor Drive, PO Box C700, West Conshohocken, PA 19428-2959. United States: ASTM International, 2016.

[33] V. Carvelli, M. Pisani and C. Poggi, "High temperature effects on concrete members reinforced with GFRP rebars," *Composites: Part B,* vol. 54, pp. 125-132, 2013.

[34] G. Fava, V. Carvelli and M. A. Pisani, "Remarks on bond of GFRP rebars and concrete," *Composites Part B,* vol. 93, pp. 210-220, 2016.

[35] M. F. Sá, A. M. Gomes, J. R. Correia and N. Silvestre, "Creep behavior of pultruded GFRP elements – Part 2: Analytical study," *Composite Structures,* vol. 93, p. 2409–2418, 2011.

[36] L. Hollaway, Polymer Composites for Civil and Structural Engineering, Dordrecht: Springer Science+Business Media , 1993.

[37] M. Bottoni, C. Mazzotti and M. Savoia, "Creep tests on GFRP pultruded specimens subjected to traction or shear," *Composite Structures,* vol. 108, pp. 514-523, 2014.

[38] F. Sarasini and C. Santulli, "Vinylester resins as a matrix material in advanced fibre-reinforced polymer (FRP) composites," in *Advanced fibrereinforced polymer (FRP) composites for structural applications*, J. Bai, Ed., Sawston, Cambridge CB22 3HJ, Woodhead Publishing Limited, 2013, p. 906.

[39] N. K. Arutyunyan, Some problems in the theory of creep, T. b. H. Nowottny, Ed., Oxford: Pergamon Press, 1966.

[40] Y. N. Rabotnov, Elements of hereditary solids mechanics, Moscow: MIR Publisher, 1980.

[41] M. A. Pisani, "Numerical analysis of creep problems," *Computers & Structures*, vol. 51, no. 1, pp. 57-63, 1994.

[42] fib, fib bulletin 40 - FRP reinforcement in RC structures, Lausanne: fib, 2007, pp.120, p. 120.

[43] T. Youssef, S. El-Gamal, E. El-Salakawy and B. Benmokrane, "Experimental Results of Sustained Load (Creep) Tests on FRP Reinforcing Bars for Concrete Structures," in *The 37th CSCE Annual Conference*, Quebec City, Quebec, Canada, 2008.

[44] M. A. Pisani, "A numerical survey on the behaviour of beams pre-stressed with FRP cables," *Construction and Building Materials*, vol. 12, pp. 221-232, 1998.

[45] P. O. Perigny, M. Robert and B. Benmokrane, "Creep rupture strength of V-Rod #3 GFRP reinforcing bars," Sherbrook University, Sherbrook, 2012.

List of Figures

List of Tables

Figure 1. Rebars tested (group 3).

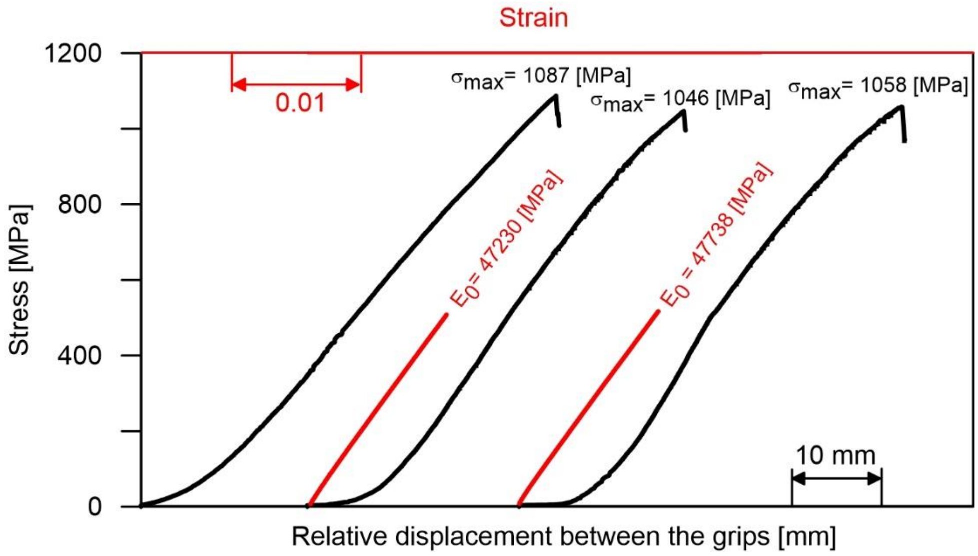

a.

b.

Figure 2. a) Results of the tensile tests (rebars of group 3) and b) photo of bars failure.

Figure 3. Testing machine used for the relaxation and creep tests.

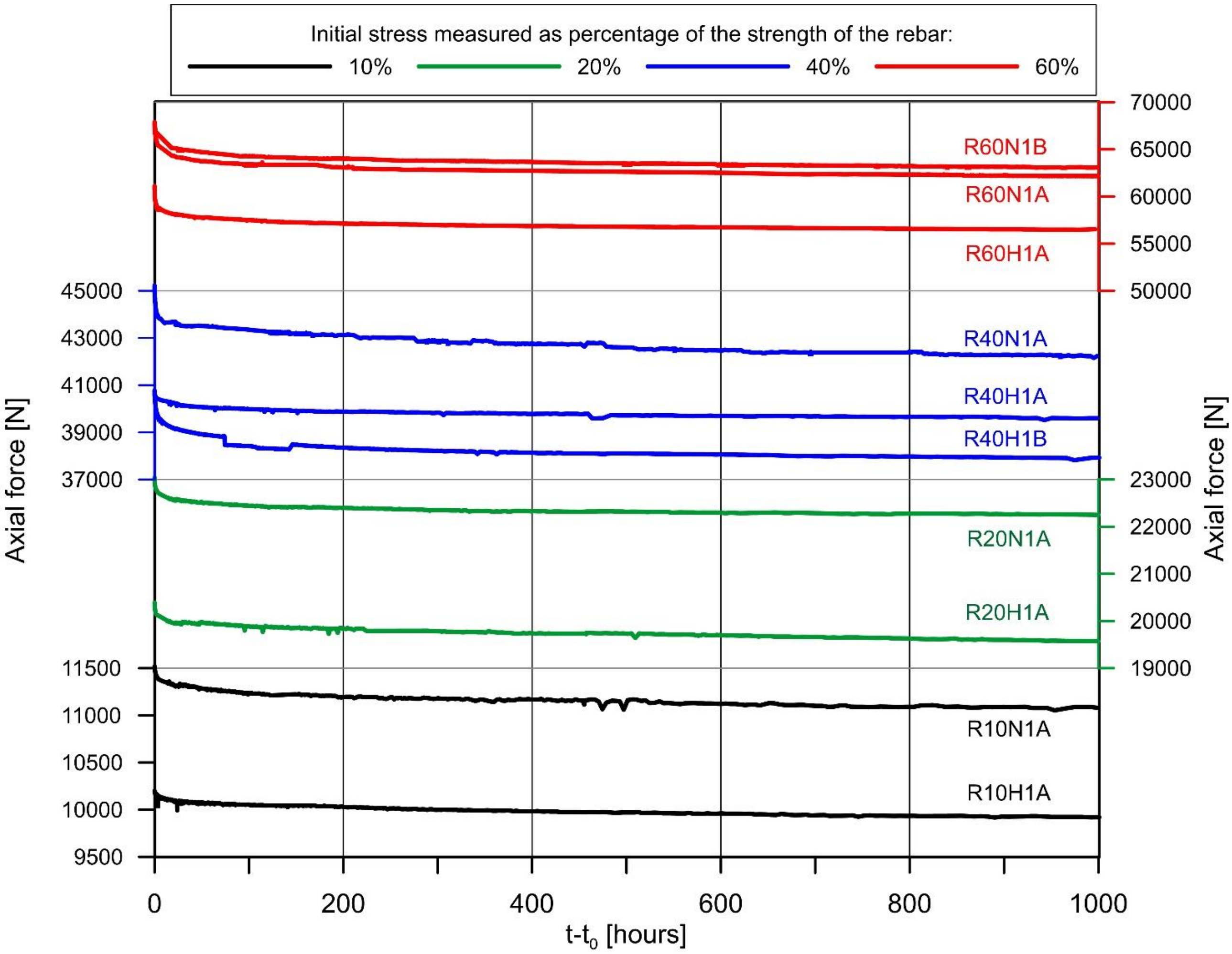

Figure 4. Results of the relaxation tests.

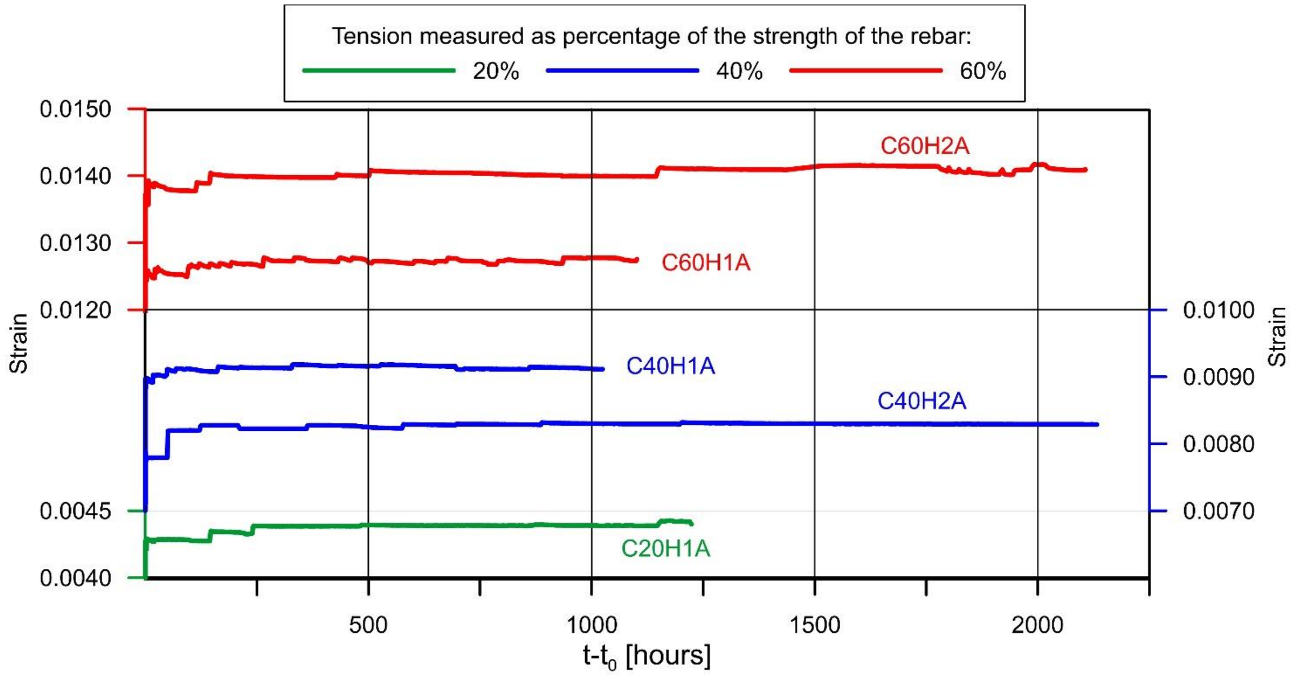

Figure 5. Results of the creep tests.

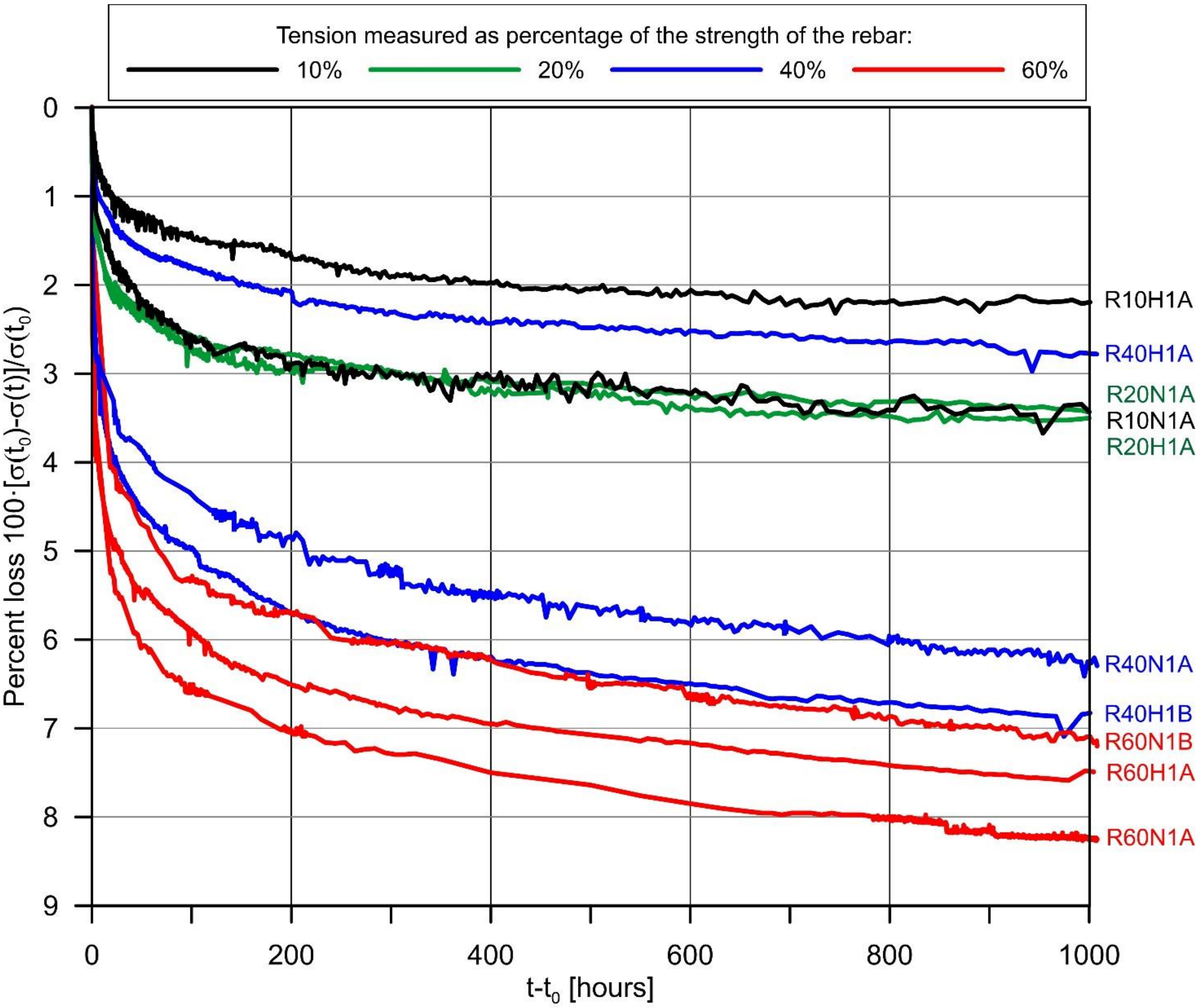

Figure 6. Relaxation tests: percent stress loss.

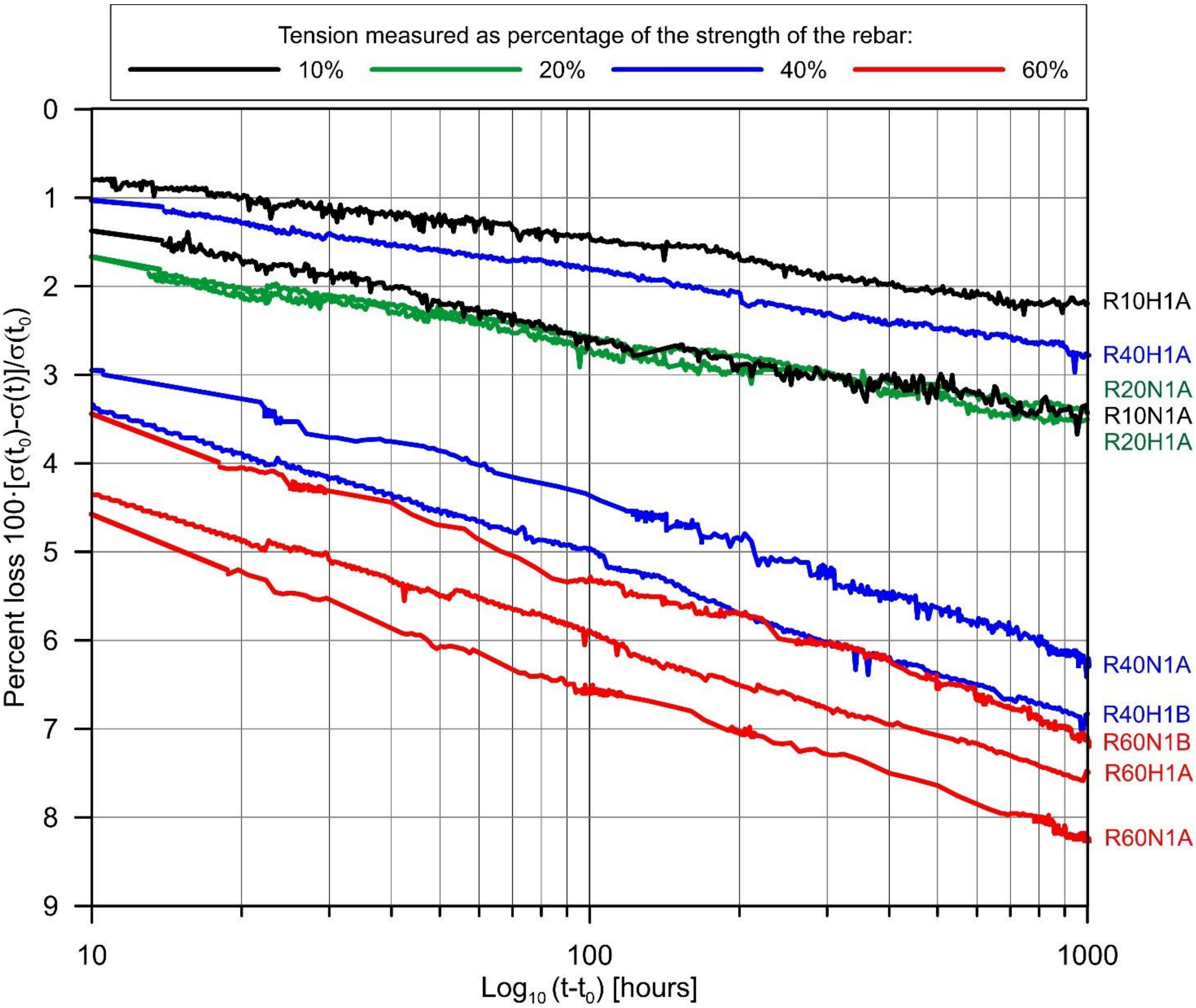

Figure 7. Relaxation tests: percent stress loss in semi-logarithmic scale.

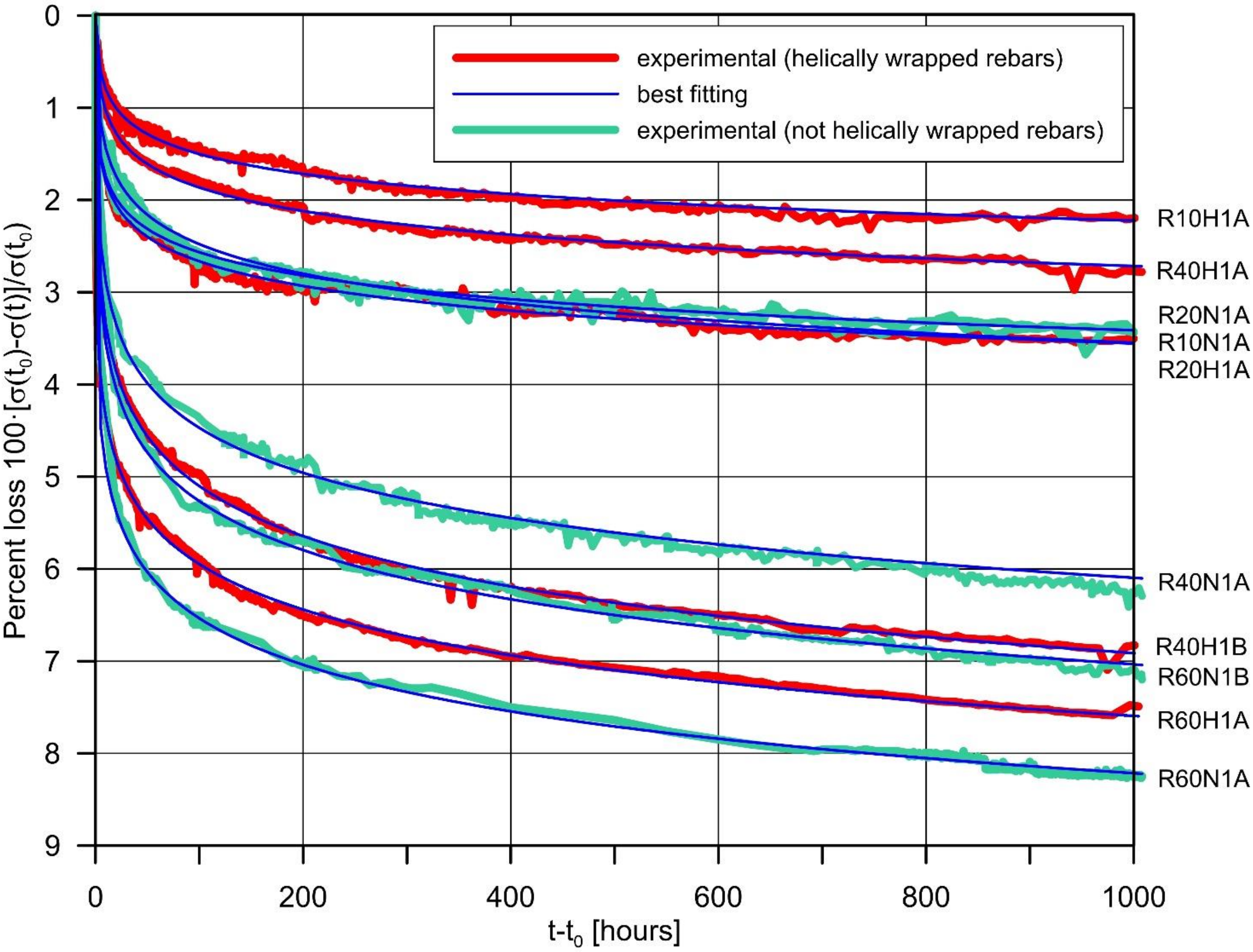

Figure 8. Relaxation tests: best fitting curves with Eq. (5).

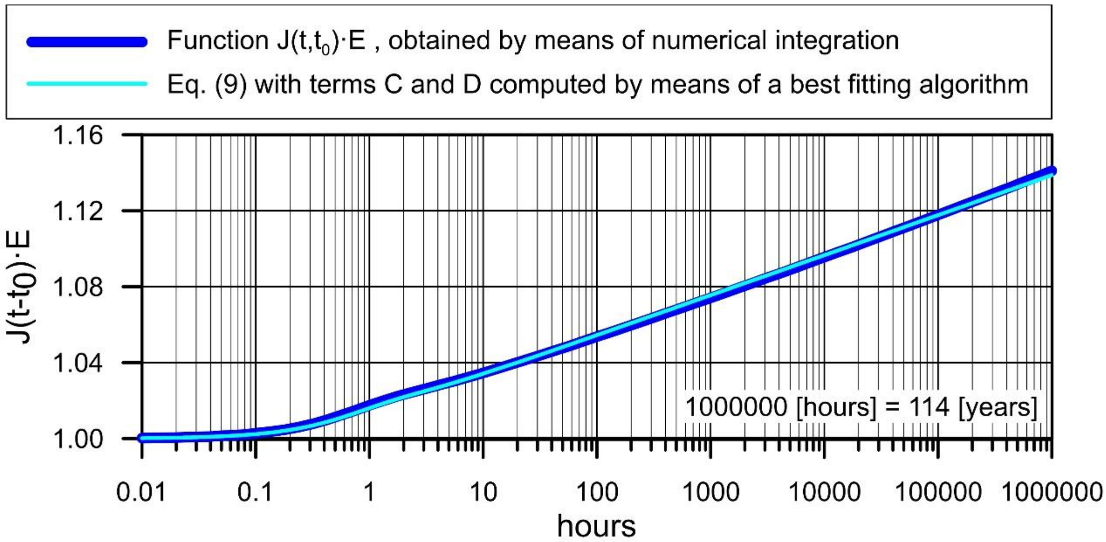

Figure 9. Function $J(t-t_0)\cdot E$ obtained by best fitting and numerical integration for R40H1B.

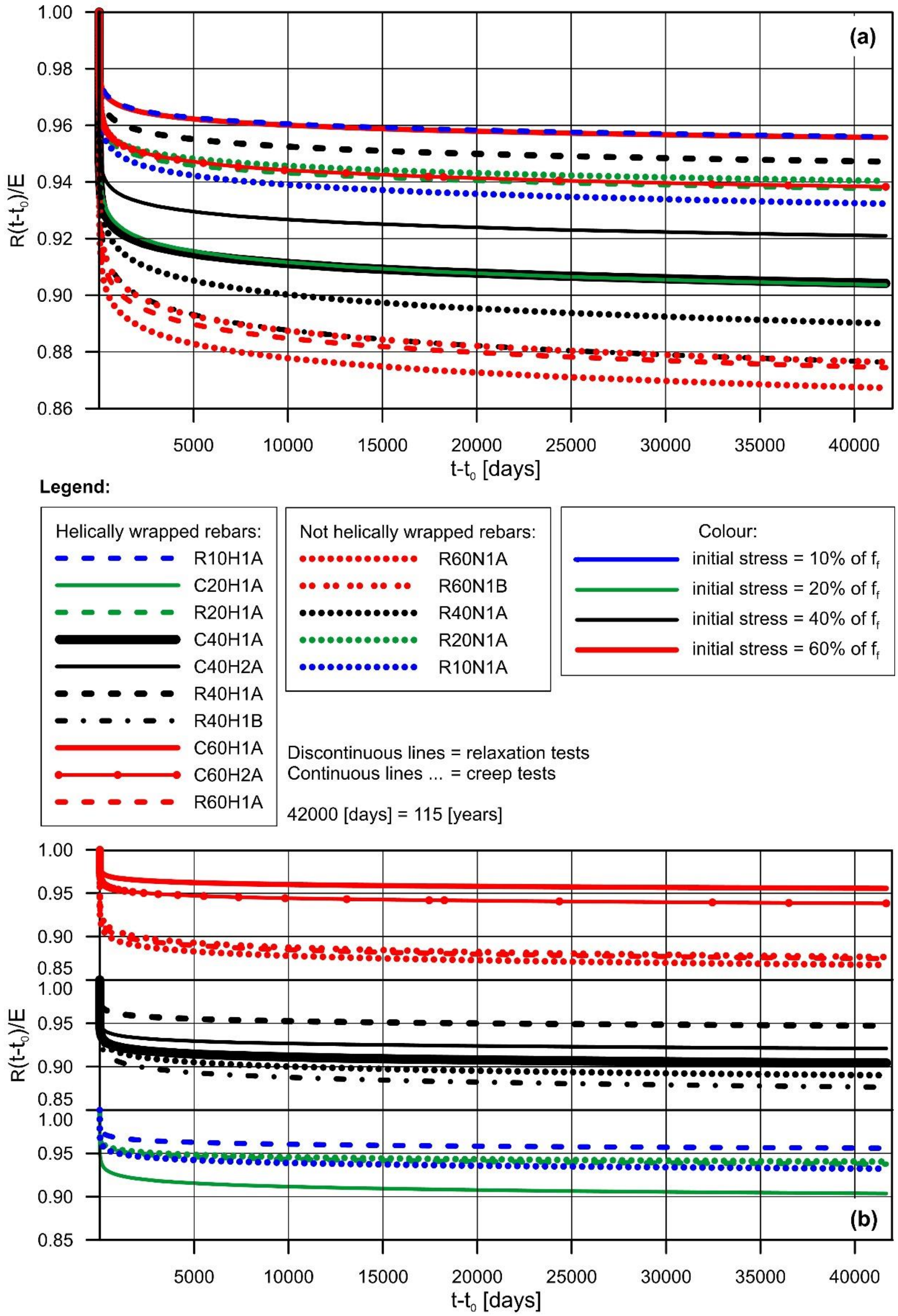

Figure 10. a) Comparison of long-term tests performed. b) Comparison between tests performed with the same initial applied stress.

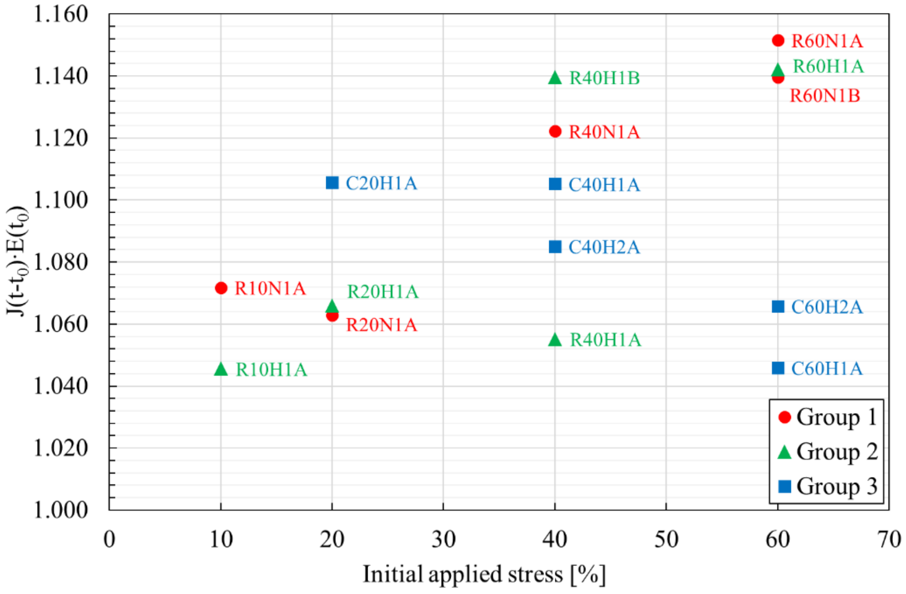

Figure 11. Ratio between the total deformation at t=100 years and the deformation at t_0 for specimens that did not fail before completion of the test.